JBC ARTICLE

# Co-targeting of CXCR4 and hedgehog pathways disrupts tumor-stromal crosstalk and improves chemotherapeutic efficacy in pancreatic cancer

Received for publication, November 1, 2019, and in revised form, April 17, 2020 Published, Papers in Press, May 1, 2020, DOI 10.1074/jbc.RA119.011748

**Mohammad Aslam Khan[1,2], Sanjeev Kumar Srivastava[1,2], Haseeb Zubair[1,2], Girijesh Kumar Patel[2], Sumit Arora[2], Moh'd Khushman[3], James Elliot Carter[1], Gregory Stephen Gorman[4], Seema Singh[1,2,5], and Ajay Pratap Singh[1,2,5,*]**

*From the [1]Department of Pathology, College of Medicine, University of South Alabama, Mobile, Alabama, [2]Department of Oncologic Sciences, Mitchell Cancer Institute, University of South Alabama, Mobile, Alabama, [3]Department of Medical Oncology, Mitchell Cancer Institute, University of South Alabama, Mobile, Alabama, [4]Pharmaceutical Sciences Research Institute, Samford University, Birmingham, Alabama, and [5]Department of Biochemistry and Molecular Biology, College of Medicine, University of South Alabama, Mobile, Alabama*

Edited by Eric R. Fearon

**Pancreatic cancer (PC) remains a therapeutic challenge because of its intrinsic and extrinsic chemoresistance mechanisms. Here, we report that C-*X*-C motif chemokine receptor 4 (CXCR4) and hedgehog pathways cooperate in PC chemoresistance via bidirectional tumor-stromal crosstalk. We show that when PC cells are co-cultured with pancreatic stellate cells (PSCs) they are significantly more resistant to gemcitabine toxicity than those grown in monoculture. We also demonstrate that this co-culture–induced chemoresistance is abrogated by inhibition of the CXCR4 and hedgehog pathways. Similarly, the co-culture–induced altered expression of genes in PC cells associated with gemcitabine metabolism, antioxidant defense, and cancer stemness is also reversed upon CXCR4 and hedgehog inhibition. We have confirmed the functional impact of these genetic alterations by measuring gemcitabine metabolites, reactive oxygen species production, and sphere formation in vehicle- or gemcitabine-treated monocultures and co-cultured PC cells. Treatment of orthotopic pancreatic tumor–bearing mice with gemcitabine alone or in combination with a CXCR4 antagonist (AMD3100) or hedgehog inhibitor (GDC-0449) displays reduced tumor growth. Notably, we show that the triple combination treatment is the most effective, resulting in nearly complete suppression of tumor growth. Immunohistochemical analysis of Ki67 and cleaved caspase-3 confirm these findings from *in vivo* imaging and tumor measurements. Our findings provide preclinical and mechanistic evidence that a combination of gemcitabine treatment with targeted inhibition of both the CXCR4 and hedgehog pathways improves outcomes in a PC mouse model.**

Pancreatic cancer (PC) is the third leading cause of cancer-related death in the United States, with an expected 57,600 new cases and 47,050 deaths in 2020 (1). It has the lowest 5-year survival rate among all cancers, which has stayed in single digit for the past several decades (2). Asymptomatic progression leading to late diagnosis as well as the lack of effective therapies are considered important factors for such a grim prognosis of PC (3). Despite recent advancements in therapeutic regimens, outcomes continue to be disappointing (4–6). Therefore, considering the continuous increase in incidence and mortality of PC, it is extremely important that we develop novel mechanism-based therapies for effective management of this devastating malignancy.

Chemoresistance in PC appears to be a highly complicated phenomenon involving both intrinsic and extrinsic mechanisms (7–11). Intrinsic resistance is attributed to the highly genetically advanced nature of pancreatic tumors that culminate into multiple overlapping and compensatory signaling pathways promoting cell survival, stemness, and drug metabolism (8, 12). On the other hand, extrinsic resistance is associated with unique histopathological characteristics of pancreatic tumors as well as paracrine signaling that is operative through bidirectional tumor-stromal crosstalk (13–17). Studies suggest that pancreatic tumor cell–derived SHH predominantly acts on PSCs and induces desmoplasia (18), whereas CXCL12 is mostly derived from activated fibroblasts and promotes growth, aggressiveness, and chemoresistance of PC cells (19–21). Pancreatic stroma is highly dense and fibrotic and considered to be an attractive therapeutic target (16, 22). However, stromal targeting has resulted in mixed therapeutic responses likely because of stromal heterogeneity and its dual impact on pancreatic tumor pathobiology. Earlier it was shown that desmoplastic tumor microenvironment acted as a barrier for drug delivery and its targeting in preclinical model led to improved therapeutic outcome (23). This approach, however, failed in clinical setting (24). Subsequent studies suggested that dense stroma keeps the tumor cells confined at the primary site and its depletion promoted tumor cell dissemination and immunosuppression (25, 26) thus necessitating deeper mechanistic investigations.

We previously demonstrated an important role of CXCR4 signaling in PC chemoresistance (20). We also showed that the gemcitabine treatment of PC cells induced CXCR4 up-regulation, providing further support for its role as a counterdefense

This article contains supporting information.

* For correspondence: Ajay Pratap Singh, asingh@health.southalabama.edu.

mechanism (10). CXCR4 is aberrantly expressed in PC cells (27, 28) and activated by stromal-derived chemokine, CXCL12, which is abundantly present in pancreatic tumor microenvironment as well as at the sites of metastases (29). In additional findings, we demonstrated that CXCL12/CXCR4 signaling engaged in forming a bidirectional tumor-stromal signaling loop by inducing the expression of sonic hedgehog (SHH), a ligand for hedgehog signaling pathway (21). SHH is shown to promote pancreatic tumor desmoplasia by inducing proliferation and differentiation of pancreatic stellate cells (PSCs) into myofibroblasts and thus impacts therapeutic outcome indirectly (23, 30).

Here we examined the therapeutic significance of co-targeting of CXCR4 and hedgehog pathways by hypothesizing their cooperative roles in tumor-stromal interaction-driven PC chemoresistance. Our findings in co-culture and orthotopic pancreatic tumor mouse models demonstrate that co-targeting of CXCR4 and hedgehog provide significant improvement in therapeutic efficacy of gemcitabine. Mechanistically, we demonstrate that the crosstalk of PC cells with PSCs leads to tumor-supportive changes in gemcitabine metabolism, anti-oxidant and stemness properties via altered gene expression, which could be reversed by targeting of CXCR4 and/or hedgehog pathways. Together, these findings provide strong preclinical evidence in support of a novel combination therapy against PC.

## Results

### *CXCR4 and hedgehog pathways mediate co-culture–induced chemoresistance of pancreatic cancer cells*

Studies from our lab and elsewhere have suggested important roles for CXCR4 and hedgehog (Hh) signaling in PC pathobiology and chemoresistance via different mechanisms (10, 20, 21, 31). Here we explored their role in mediating the chemoresistance of PC cells when co-cultured with PSCs. We treated the monocultures and co-cultures with gemcitabine in the presence or absence of CXCR4 antagonist (AMD3100) and/or hedgehog inhibitor (GDC-0449) and measured the viability of PCCs. Inhibition of either CXCR4 or Hh sensitized the PCCs to gemcitabine toxicity in co-culture (Fig. 1*A* and Fig. S1). Notably, combined inhibition of CXCR4 and Hh pathways led to a nearly complete abolition of co-culture–induced chemoresistance. Importantly, these effects of combination therapy were synergistic in nature when compared with the single-drug treatments (Table S1). No significant effect of CXCR4 and/or Hh inhibition, however, was recorded on gemcitabine toxicity of PCCs in monocultures. Moreover, treatment of AMD3100 and GDC-0449 alone or in combination had no significant effect on the viability of Colo357 cells in monocultures or co-cultures without gemcitabine treatment (Fig. 1*A*). These findings were further confirmed by performing live/dead cell assay using ethidium homodimer-1 (EthD-1) and Calcein AM staining and poly (ADP-ribose) polymerase (PARP) cleavage. Reduced tumor cell death (lesser EthD-1 red fluorescence positivity) was observed in co-culture treated with gemcitabine than those grown in monoculture, and as expected, co-treatment with AMD3100 and/or GDC-0449 promoted cell killing by gemcitabine in co-cultured PCCs (Fig. 1*B*). Similarly, an increased signal of cleaved PARP was also reported in PCCs co-treated with gemcitabine and AMD3100 and/or GDC-0449, compared with those treated with gemcitabine alone (Fig. 1*C*). To further confirm the role of CXCR4 and Hh signaling in chemoresistance, we silenced CXCR4 and SMO (important mediator of hedgehog signaling) expression by RNAi in both PCCs (MiaPaCa and Colo357) and PSCs (Fig. 1*D*). CXCR4- and/or SMO-silenced PCCs, co-cultured with PSCs, were treated with gemcitabine, and their cell viability was determined. We observed that the silencing of CXCR4 alone or in combination with SMO significantly reduced their viability when treated with gemcitabine compared with control scrambled siRNA-treated cells (Fig. 1*E*). To further support a cooperative role of PSCs in co-culture–induced chemoresistance, we used an additional PSC line. The resulting data (Fig. S2) are consistent with findings presented here. We next determined the effect of PSC co-culture with PCCs on their activation status by examining the expression of α-SMA, a myofibroblast marker, and in the presence of lipid droplets. Our results in two PSCs lines show that co-culture with PCCs activates PSCs as evident by increased expression of α-SMA (Fig. 2*A*) and reduced accumulation of lipid droplets (Fig. 2*B*). We also monitored the effect of CXCR4 and Hh inhibition on the viability of PSCs in monoculture and co-culture with PCCs. Our data demonstrate that the inhibition of Hh either by GDC-0449 or SMO silencing significantly reduces PSCs viability in co-culture. However, inhibition of CXCR4 had a marginal effect only on PSCs viability (Fig. 2, *C* and *D*). To determine the contribution of CXCR4 and Hh signaling inhibition in PSCs on the chemoresistance of PC cells, we co-cultured PCCs with CXCR4- and/or SMO-silenced PSCs and treated them with gemcitabine. The data demonstrate that the silencing of SMO in PSCs effectively abolished co-culture–induced chemoresistance (Fig. 2*E*). CXCR4 silencing alone n PSCs, however, did not have a significant effect.

### *CXCR4 and hedgehog pathways mediate co-culture–induced expression of chemoresistance-associated genes*

To elucidate the underlying mechanisms of co-culture–induced chemoresistance in PCCs, we carried out pathway-focused gene expression analyses. We observed that in PCCs co-cultured with PSCs, expression of a number of genes associated with gemcitabine metabolism, antioxidant, and stemness altered (Fig. 3*A*). Specifically, MiaPaCa cells in co-culture had an up-regulation of *NT5C1A* encoding for cytosolic 5–nucleotidase I A, an enzyme which dephosphorylates gemcitabine monophosphate into gemcitabine. On the other hand, Colo357 cells in co-culture exhibited an increase in the expression of *CDA*, which encodes for cytidine deaminase, an enzyme that converts gemcitabine into 2′,2′-difluorodeoxyuridine. Moreover, expression of *dCK*, encoding deoxycytidine kinase required for conversion of gemcitabine into active metabolite, decreased in both the cell lines when co-cultured with PSCs. Furthermore, significant up-regulation of genes encoding for antioxidant enzymes such as GSH peroxidases *GPXs*, and nuclear factor E2-related factor 2 (*NRF-2*) was observed in both the cell lines. In addition, stemness-associated genes, *SOX2* and *OCT4,* were up-regulated in MiaPaCa cells

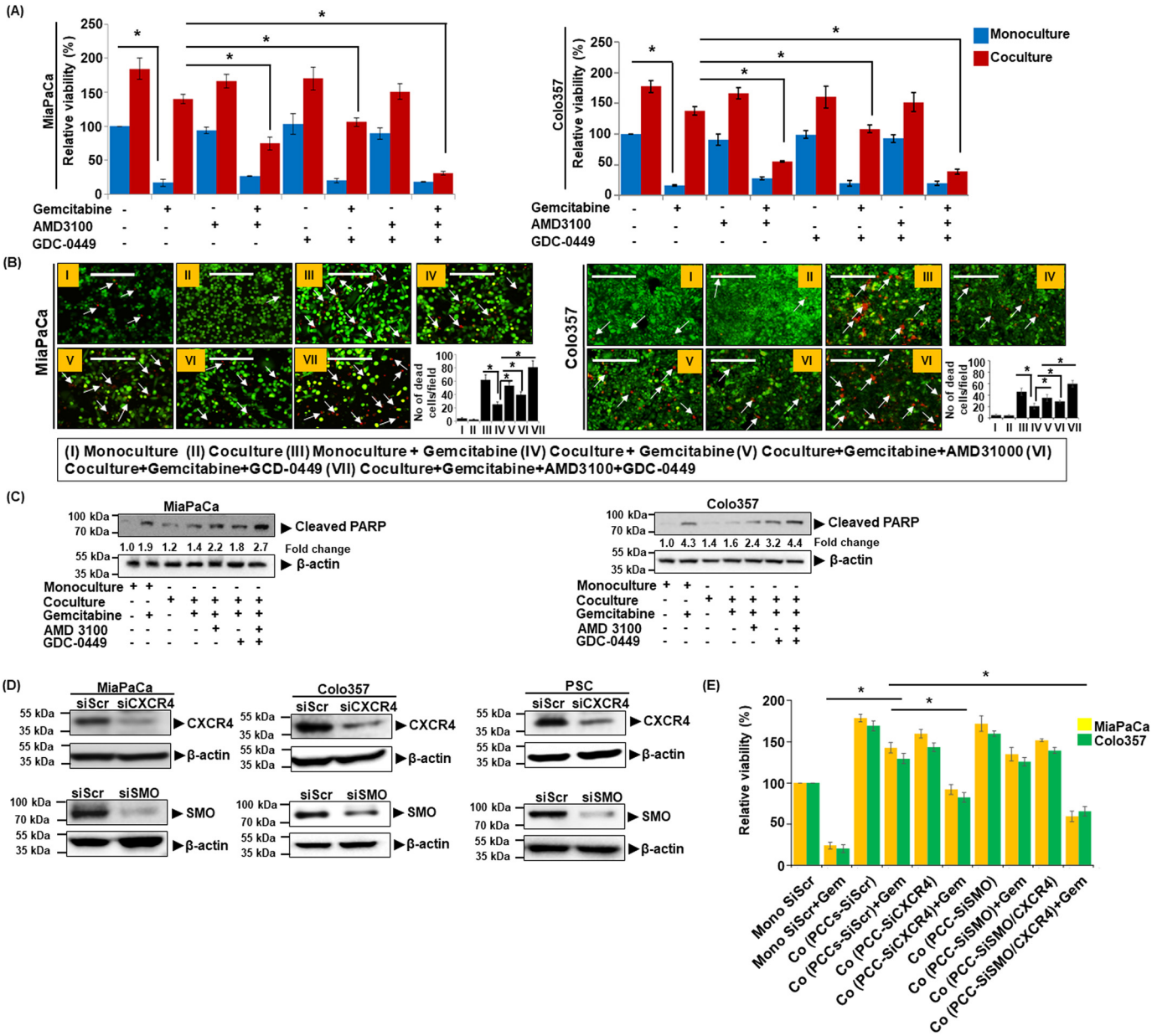


**Figure 1. Co-culture induces chemoresistance in pancreatic cancer through CXCR4 and hedgehog pathways.** *A*, monoculture of PC cells (MiaPaCa or Colo357) or co-culture with PSCs were treated with gemcitabine (5 $\mu$M) alone and in combination with AMD3100 (5 $\mu$g/ml) and GDC-0449 (5 $\mu$M) for 96 h. Thereafter, viable cells counted and presented as relative percentage viability. *Bars* represent the average of triplicates ± S.D. *, $p < 0.05$. *B*, gemcitabine-treated PC cell monoculture and PCC. PSC co-culture in the presence or absence of AMD3100 and/or GDC-0449 and cells were stained with Calcein-AM (*green fluorescence*) and ethidium homodimer-1 (*red fluorescence*). Photographs were taken under fluorescence microscope. *Arrows* indicate ethidium homodimer-1–positive dead cells. The number of dead cells was counted in 10 random fields and presented as mean ± S.D. *, *p* value <0.05. *Scale bar* is 200 $\mu$m. *C*, similarly as in *B*, at the end of treatment, total protein was isolated from the harvested PC cells and expression of cleaved PARP determined by immunoblotting. $\beta$-actin was used as an internal control. Fold change shows the level of cleaved PARP expression after normalizing with $\beta$-actin. *D*, pancreatic cancer cells were transiently transfected with either scrambled (*siScr*) or CXCR4 (*siCXCR4*) or SMO (*siSMO*)-targeting siRNA and CXCR4 and SMO silencing was confirmed by immunoblotting. *E*, CXCR4- and/or SMO-silenced PCCs were co-cultured with PSCs and treated with gemcitabine (5 $\mu$M) for 96 h. Viable cells were counted and data presented as relative percentage viability. *Bars* represent the average of triplicates ± S.D. *, $p < 0.05$.

co-cultured with PSCs, whereas Colo357 cells exhibited altered expression of *SOX2* and *KLF-4* as compared with those grown in monoculture (Fig. 3*A*). To examine the role of CXCR4 and Hh pathways in mediating these gene expression changes, we performed qRT-PCR on RNAs isolated from PCCs in co-cultures following treatment with AMD3100 and GDC-0449, alone or in combination. We observed that the inhibition of CXCR4 and Hh pathways cooperatively led to the abrogation of co-culture–induced up-regulation and down-regulation of *NT5C1A* and *dCK*, respectively, in MiaPaCa cells. On the other hand, inhibition of either CXCR4 or Hh alone did not alter the co-culture–induced down-regulation of *dCK*, but their combined inhibition led to regained expression of *dCK* in Colo357 cells. Interestingly, inhibition of CXCR4 either alone or in combination with Hh abrogated co-culture–induced *CDA* up-regulation in Colo357 cells, whereas co-culture–induced up-regulation of *NRF-2* and *GPX-1* was significantly inhibited upon blocking of CXCR4 and/or Hh pathways in MiaPaCa cells

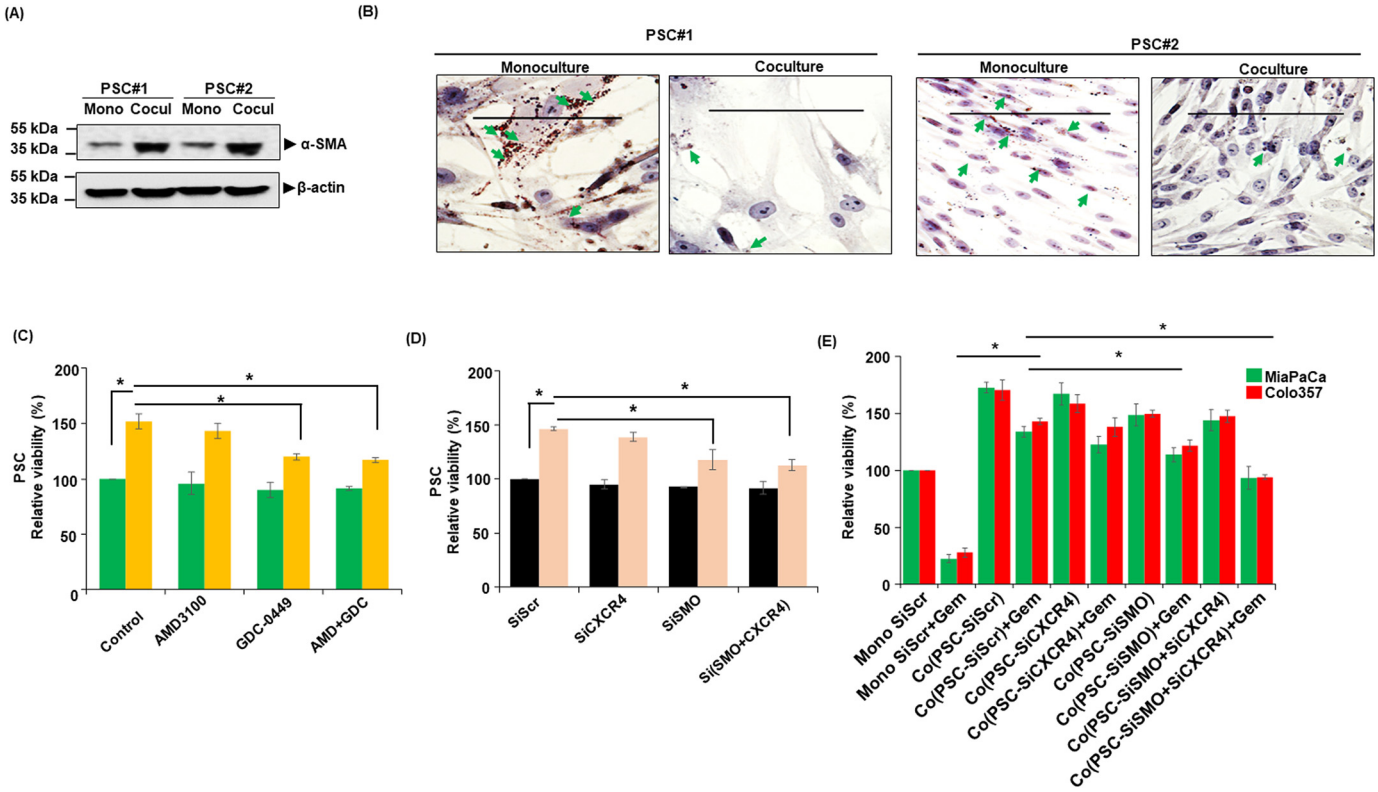


**Figure 2. Activation status of PSCs in monoculture and co-culture system and effect of CXCR4 and Hh inhibition in co-culture on PSC survival and chemoresistance of pancreatic cancer cells.** *A*, two different types of PSCs (PSC#1 and PSC#2) were co-cultured with PCCs and activation of PSCs was determined by checking α-SMA expression through immunoblotting. β-actin was used as loading control. *B*, lipid droplet staining in monoculture and co-culture PSCs was performed using Oil Red O staining and images taken under bright field microscope. *Arrows* indicate presence of lipid droplets in PSCs. *Scale bar* is 100 μm. *C*, monoculture (PSC) or co-culture (PSCs with PCCs) was established and treated with AMD3100 (5 μg/ml) and/or GDC-0449 (5 μM) for 96 h and viable cells were counted. Data are presented as relative percentage viability. Mean ± S.D., $n = 3$; *, $p < 0.05$. *D*, CXCR4 or SMO expression was silenced by RNAi (data not shown) in PSCs and then monoculture (PSCs) or co-culture (PSCs with PCCs) was established and cell viability determined. The data are presented as relative percentage viability. Mean ± S.D., $n = 3$; *, $p < 0.05$. *E*, CXCR4 and/or SMO silenced PSCs were co-cultured with PCCs and treated with gemcitabine (5 μM) for 96 h. Viable cells were counted and data presented as relative percentage viability. *Bars* represent the average of triplicates ± S.D.; *, $p < 0.05$.

(Fig. 3*B*). Similarly, *NRF-2* up-regulation was inhibited in the presence of AMD3100 alone or in combination with GDC-0449 but no significant effect was observed upon GDC-0449 treatment alone in Colo357 cells. Additionally, co-culture–induced *GPX-1* up-regulation was significantly inhibited in AMD3100- and/or GDC-0449-treated Colo357 cells. Inhibition of CXCR4 and/or hedgehog pathways also inhibited *SOX2* expression, whereas *OCT4* up-regulation was significantly blocked upon combination treatment of AMD3100 and GDC-0449 in MiaPaCa cells. Interestingly, inhibition of CXCR4 alone or in combination with hedgehog pathway effectively suppressed co-cultured–induced *SOX2* and *KLF-4* up-regulation in Colo357 cells (Fig. 3*B*). To further confirm the involvement of CXCR4 and SHH signaling pathways in these co-culture–induced changes, PCCs were treated with recombinant CXCL12 and/or SHH, and changes in gene expression analyzed. Data demonstrated that the treatment of CXCL12 caused most of the changes in gene expression, suggesting an indirect role of Hh pathway (Fig. 3*C*). To further confirm the involvement of CXCR4 and Hh pathway in altered gene expression, we examined gene expression changes in CXCR4- or SMO-silenced PCCs treated with CXCL12 or SHH, respectively. The data demonstrate that CXCL12-mediated down-regulation of *dCK* and up-regulation of *NT5C1A*, *NRF-2*, and *SOX-2* is significantly abrogated in CXCR4-silenced cells (Fig. 3*D*). SMO-silencing did not have a major effect on gene expression further suggesting its indirect role in chemoresistance through activation of PSCs.

### *Inhibition of CXCR4 and hedgehog pathways alters gemcitabine metabolism, ROS levels, and stemness*

To confirm if altered gene expression translates into changes in gemcitabine metabolism and ROS generation, we measured their levels in PCCs by LC-tandem MS and H2DCFDA staining, respectively. We observed an enhanced accumulation of dFdCTP in monocultured PCCs as compared with those co-cultured with PSCs. Remarkably, inhibition of CXCR4 and/or hedgehog pathways significantly enhanced dFdCTP accumulation in co-cultured PCCs (Fig. 4*A*). In contrast, accumulation of gemcitabine was higher in co-cultured PCCs, compared with those in monoculture, which was significantly reduced upon blocking CXCR4 and/or hedgehog pathways (Fig. 4*B*). Next, our flow cytometry data demonstrated reduction in basal as well as gemcitabine-induced ROS generation in co-cultured PCCs as compared with PC cells in monoculture (Fig. 4*C*). Furthermore, we observed that the blocking CXCR4 and hedgehog pathway alone or in combination abrogated the inhibitory effect of co-culture on ROS generation. Next, we examined the

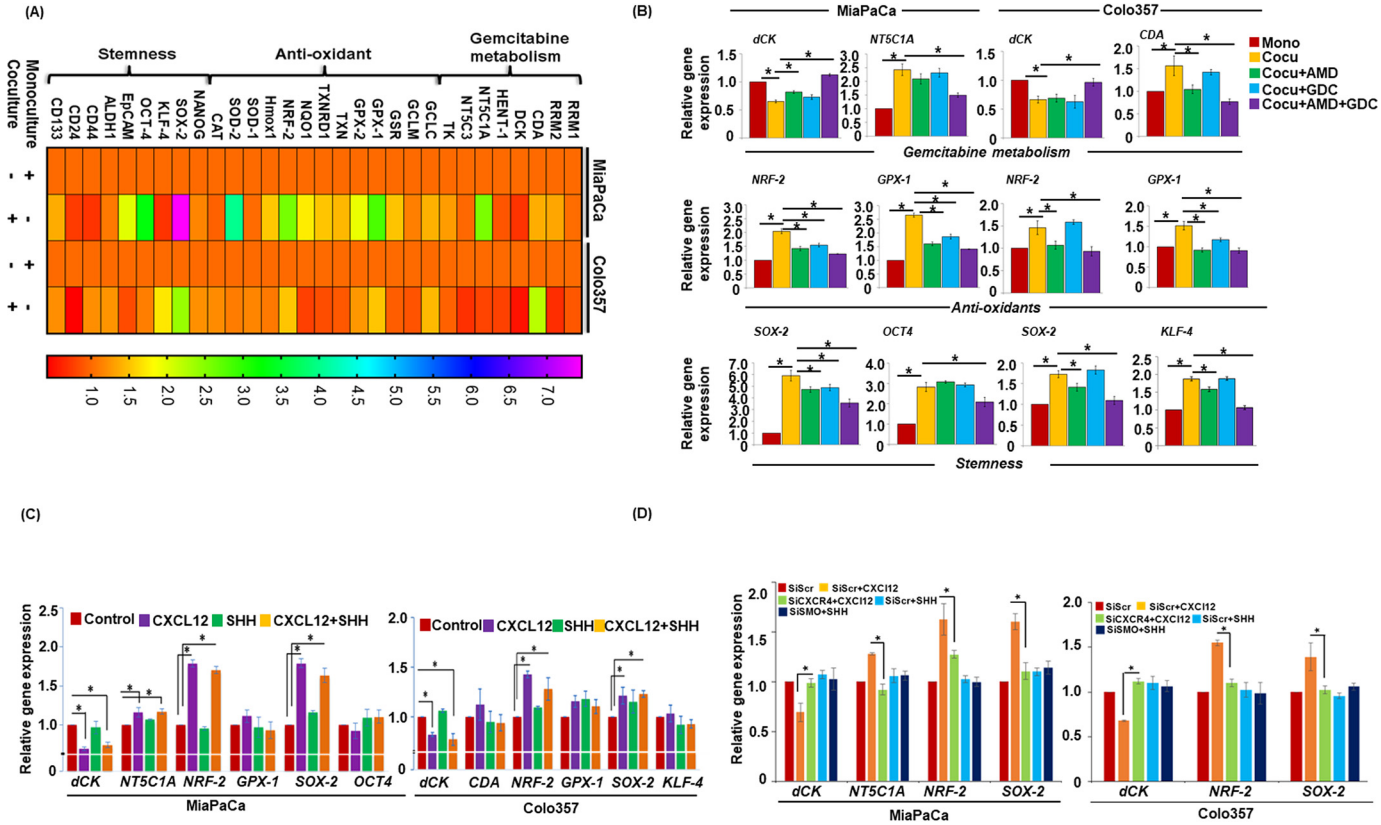


**Figure 3. Activation of CXCR4 and hedgehog pathways alters gene expression of associated with gemcitabine metabolism, anti-oxidant and stemness in pancreatic tumor cells.** *A*, monoculture or co-culture system was established. Total RNA was isolated from PC cells and subjected to qRT-PCR array analysis to examine gene expression. Monoculture of PC cells was used as control. *B*, co-culture of PCCs and PSCs was established and treated with AMD3100 (5 $\mu$g/ml) and/or GDC-0449 (5 $\mu$M) for 24 h. Afterward RNA was isolated, cDNA was prepared, and expression of gemcitabine metabolism (dCK, NT5C1A, and CDA), anti-oxidant (NRF-2 and GPX-1), and stemness (SOX-2, OCT4, and KLF-4) associated genes was examined using qRT-PCR. Monoculture of PCCs (MiaPaCa or Colo357) was taken as control and GAPDH served as an internal control for expression analysis. *, $p < 0.05$. *C*, monoculture of PCCs was treated with SHH (2.0 $\mu$g/ml) and/or CXCL12 (100 ng/ml) for 24 h. Afterward RNA was isolated; cDNA was prepared; and expression of gemcitabine metabolism, anti-oxidant, and stemness-associated genes was checked using qRT-PCR. *D*, expression of *dCK, NT5C1A, GPX-1, NRF-2, SOX-2* and *KLF-4* was examined in CXCR4- and SMO-silenced cells after treatment with SHH (2.0 $\mu$g/ml) or CXCL12 (100 ng/ml) for 24 h. *Bars* represent the average of triplicates ± S.D.; *, $p < 0.05$.

role of CXCR4 and hedgehog pathways in co-culture–induced stemness of PCCs by monitoring the sphere-forming ability on ultra-low attachment surface plates. Monoculture and co-culture (with PSCs) of PCCs were established and treated with AMD3100 and/or GDC-0449 in the presence and absence of gemcitabine. Thereafter, PCCs were plated on ultra-low attachment surface wells and inserts containing PCCs or PSCs were placed over. Sphere formation was visualized under microscope after 7 days, which showed greater sphere-forming capacity of PCCs in co-culture as compared with that in monoculture. Interestingly, gemcitabine-treated PCCs exhibited enhanced stemness in both monocultures and co-cultures. Dual inhibition of CXCR4 and hedgehog pathways resulted in reduced formation of spheres, whereas inhibition of either CXCR4 or hedgehog pathway alone did not have any significant effect (Fig. 4*D*).

### *Co-targeting of CXCR4 and hedgehog pathways enhances chemotherapeutic response in vivo*

To obtain the direct evidence *in vivo*, we evaluated the therapeutic efficacy of gemcitabine alone and in combination with AMD3100 and/or GDC-0449 in nude mice. Luciferase-tagged MiaPaCa cells mixed with PSCs were injected into the tail of the pancreas of nude mice and tumor formation monitored each alternate day by palpation. After 1 week, when tumors became palpable, mice were randomly divided into eight treatment groups (vehicle, gemcitabine, AMD3100, GDC-0449, AMD3100 + GDC-0449, gemcitabine + AMD3100, gemcitabine + GDC-0449, gemcitabine + AMD3100 + GDC-0449). Treatments continued for 2 weeks and all mice were sacrificed after a week interval (Fig. 5*A*). At day 0 (treatment initiation) and each subsequent week, tumor growth was monitored by noninvasive *in vivo* imaging (Fig. 5, *B* and *C*). As expected, the treatment of mice with gemcitabine resulted in reduction of tumor growth, compared with those treated with vehicle only. Mice treated with AMD3100 alone or in combination with GDC-0449 (without gemcitabine) showed slower tumor development as compared with those treated with GDC-0449 only. Furthermore, treatment of mice with gemcitabine in combination with either AMD3100 or GDC-0449 had improved therapeutic efficacy, compared with gemcitabine alone. Combination of gemcitabine with AMD3100 had superior effect than that with GDC-0449, which was also confirmed by end-point tumor measurement analysis (Fig. 5, *D* and *E*). Remarkably, triple combination of gemcitabine, AMD3100 and GDC-0449 had a tremendous effect on the tumor growth compared with any other treatment group as recorded in noninvasive imaging and end-point anal-

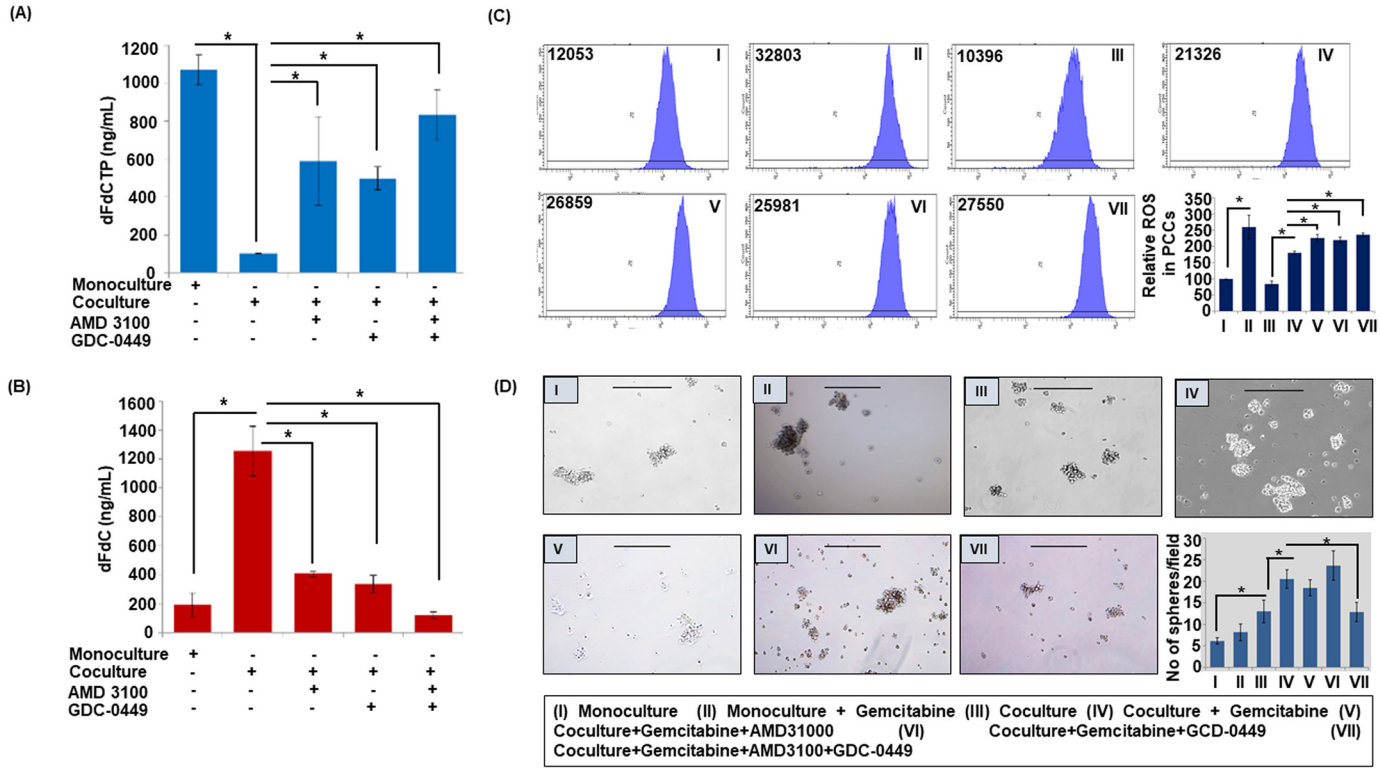


**Figure 4. Co-culture alters gemcitabine metabolism, ROS generation and pancreatic cancer stemness.** *A–B*, co-culture of pancreatic tumor cells and pancreatic stellate cells was established and treated with AMD3100 and/or GDC-0449 for 48 h and gemcitabine (5 $\mu$M) was added 4 h prior to end of incubation. Cells were harvested and samples were subjected to LC-MS/MS for the analysis of gemcitabine triphosphate and gemcitabine accumulation in tumor cells. *C*, monoculture of PCCs was treated with gemcitabine for 24 h and established co-culture was pretreated with AMD3100 and/or GDC-0449 for 24 h followed by gemcitabine treatment for 24 h. After end of incubation, cells were washed and incubated with DCFDA (20 $\mu$M) for 30 min and analyzed for ROS level through flow cytometry. *D*, monoculture treated with vehicle or gemcitabine or co-culture system was treated with vehicle, gemcitabine alone, or in combination with AMD3100 and/or GDC-0449 for 48 h. After that cells were trypsinized, counted, and 1000 cells/well were plated in ultra-low attachment plate and insert containing PCCs or PSCs kept over the plated cells. Plates were incubated for 7 days to form spheres and they were imaged under bright field microscope and number of spheres was counted and presented in graph as average number of spheres in each combination ± S.D. *, $p < 0.05$. *Scale bar* is 250 $\mu$m.

ysis of resected tumor xenografts (Fig. 5, *B–E*). A comparison of the efficacy of different treatments suggested that the combination therapy provided synergistic outcomes (Table S2). Next, we performed hematoxylin and eosin (H&E) staining and immunohistochemical analyses (Ki67 and cleaved caspase-3) on tumor sections from different treatment group mice (Fig. 6, *A–C*). Our H&E data suggested extensive desmoplasia in vehicle-treated mice and degree of desmoplasia reduces upon AMD3100 and/or GDC-0449 treatment and is completely abolished in mice treated with gemcitabine along with AMD3100 and GDC-0449. Ki67 staining (a measure of cell proliferation) was reduced in tumor sections from gemcitabine-treated mice, compared with those treated with vehicle only. In addition, mice treated with AMD3100 and/or GDC-0449 also showed reduction in number of proliferative tumor cells. Combination of gemcitabine with AMD3100 and/or GDC-0449 showed greater reduction in Ki67-positive cells compared with mice treated with gemcitabine with most remarkable reduction observed in triple combination–treated mice (Fig. 6*B*). Tumor sections from gemcitabine-treated mice also showed increased cleaved caspase-3 staining, compared with those from vehicle-treated mice, and the most robust increase in caspase-3 activation was recorded in tumor sections from combined-treatment group (AMD3100, GDC-0449, and gemcitabine) mice (Fig. 6*C*).

## Discussion

Pancreatic cancer has remained a therapeutic challenge despite our improved understanding of genetics and molecular pathways involved in its etiology and aggressive progression (3, 32). Here we demonstrated that CXCR4/CXCL12 and hedgehog signaling pathways play an important role in mediating the chemoresistance of PC cells upon co-culturing with PSCs. We identified altered gemcitabine metabolism, ROS production, and induction of cancer stemness as important underlying mechanisms. Combined targeting of CXCR4 and hedgehog pathways with chemotherapy almost entirely stalled pancreatic tumor growth in an orthotopic mouse model of PC providing a direct evidence for their therapeutic significance.

We first focused on investigating the direct roles of CXCR4 and hedgehog pathways, alone and in concert, in mediating the tumor-stromal interaction-driven chemoresistance of PC. For this, we utilized co-culture model to establish bidirectional crosstalk between PC cells and PSCs. We found that the treatment of CXCR4 antagonist, AMD3100 and/or hedgehog inhibitor, GDC-0449, efficiently reduced co-culture–induced gemcitabine resistance in PCCs. We also observed that the targeting of CXCR4 was more effective than hedgehog inhibition in causing the chemosensitization of PC cells and their co-targeting nearly abolished co-culture–induced chemoresistance. This is

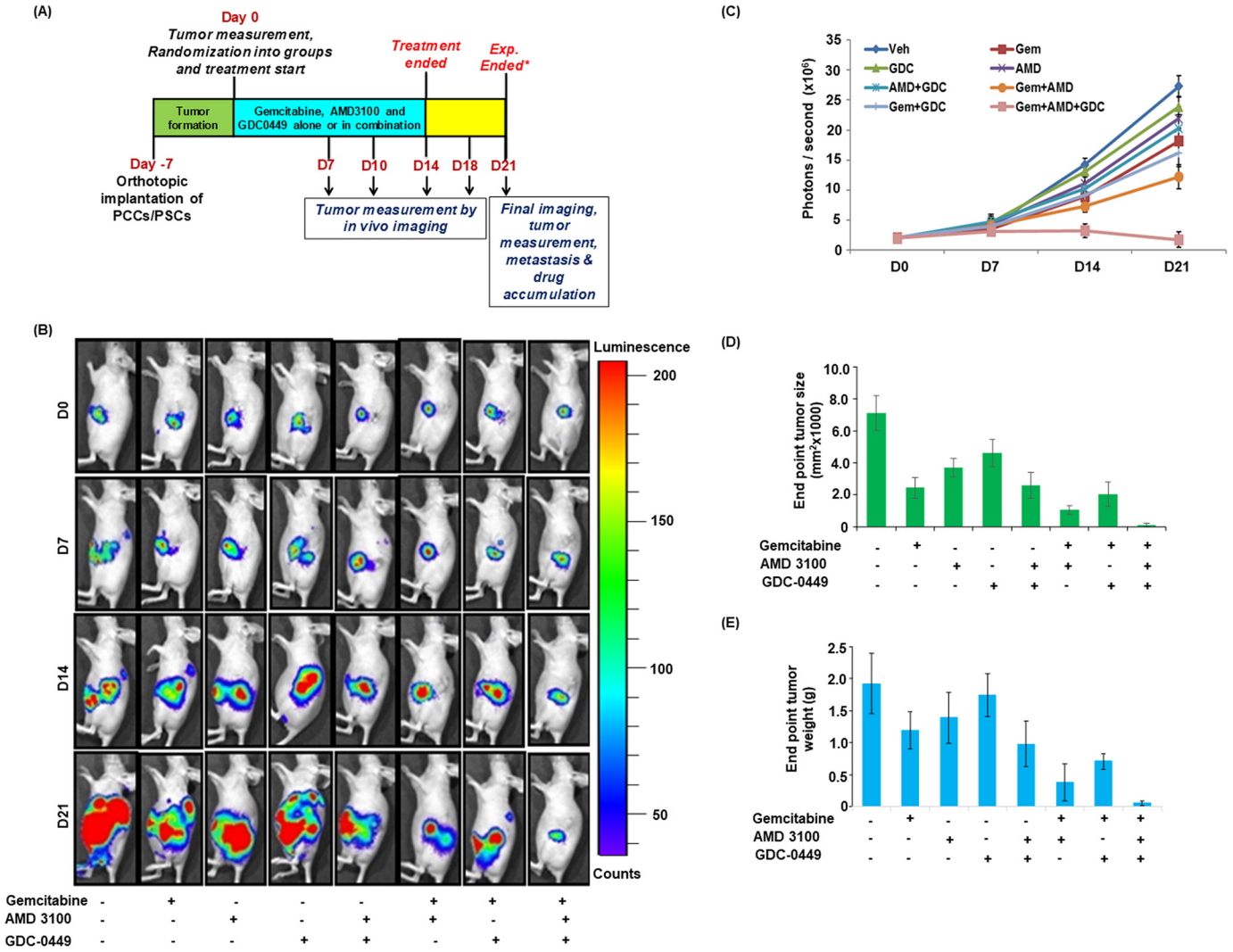


**Figure 5. Administration of CXCR4 antagonist and hedgehog inhibitor potentiated anti-tumor efficacy of gemcitabine in orthotropic xenograft tumor model.** *A*, schematic diagram of treatment strategy in orthotopic xenograft model. *B* and *C*, tumor growth in different treatment groups of mice was monitored by measuring luminescence at different time intervals using IVIS imaging station following i.p. injection of D-Luciferin (150 mg/kg). Images are representative of mice from all the treatment groups at different time point. *D* and *E*, at the end point, animals were sacrificed, tumors were resected, and tumor size (*D*) and weight (*E*) were measured. Tumor volume was calculated by using the formula (A × B2)/2, where A is the larger and B is the smaller of the two dimensions.

in line with our prior observation where treatment with exogenous CXCL12 conferred chemoresistance to PC cells via activation of survival signaling (20). In addition, CXCR4 up-regulation occurred upon gemcitabine treatment of PC cells in a counterdefense against chemotherapy (10). Interestingly, our data also supported that PSCs play a significant and direct role in promoting PC chemoresistance besides indirectly impacting therapeutic outcome via promotion of tumor desmoplasia leading to restricted drug delivery (16, 23). These observations were further validated in animal studies where we established orthotopic pancreatic tumor xenografts via co-injection of PCCs and PSCs and treated with gemcitabine alone or in combination with AMD3100 and/or GDC-0449. These inhibitors are shown to be effective in mice in previous studies (33, 34). Furthermore, orthotopic implantation of SHH-expressing primary human pancreatic epithelial and cancer cells induce desmoplasia in mice (18). Thus, our current findings provide support for a cooperative role of CXCR4 and hedgehog pathways in establishing a bidirectional tumor-stromal crosstalk that has pathobiological significance in growth and chemoresistance of PC cells.

From the mechanistic standpoint, our data demonstrated that the co-culture of PCCs with PSCs altered the expression of several genes associated with gemcitabine metabolism, ROS generation, and cancer stemness. Several of these genes were indeed found to be regulated through the cooperative action of CXCR4 and hedgehog signaling pathways. Importantly, the rate-limiting enzyme of gemcitabine activation (35), dCK found to be reduced in PC cells co-cultured with PSCs. dCK expression is positively co-related with overall survival and disease-free survival in PC patients (36). A recent study has also suggested that the forced expression of dCK in PC cells inhibits tumor cell proliferation and aggressiveness (37). Other two enzymes that were altered in cell-specific manner were *NT5C1A* and *CDA*. The dephosphorylating enzyme NT5C1A converts gemcitabine monophosphate into gemcitabine and is

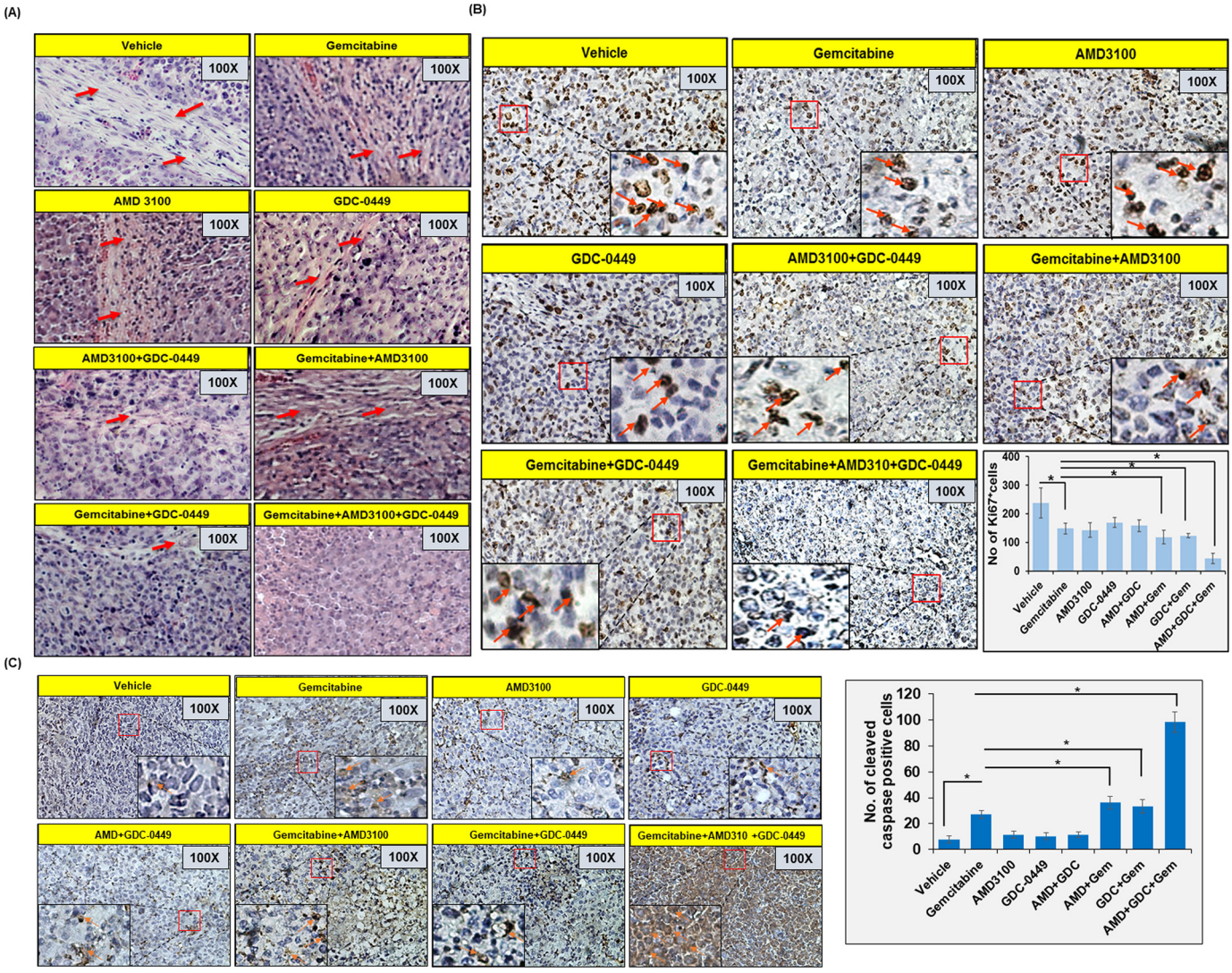


**Figure 6. Immunohistochemistry analysis in pancreatic tumors.** *A*, tissue sections of orthotopically developed pancreatic tumors were deparaffinized, rehydrated, and stained with H&E to study their histopathological characteristics. Desmoplastic region is depicted with *red arrows*. *B* and *C*, tumor sections were also stained with Ki67 (*B*) and cleaved caspase-3 (*C*). Representative images show predominantly nuclear and cytoplasmic staining of Ki67 and caspase-3, respectively. All images have been taken at 100 × and 400 × (*inset*) magnification. *Bars* in the graphs represent average number of stained cells from five random fields or both ± S.D.; *, $p < 0.05$.

reported to be overexpressed in PC (38, 39). On the other hand, CDA is a gemcitabine catabolizing enzyme that converts gemcitabine into 2′,2′-difluoro-deoxyuridine leading to its reduced cellular toxicity (40). In a preclinical study, nab-paclitaxel was shown to degrade CDA as a synergistic therapeutic mechanism with gemcitabine (41). In another study, tumor-associated macrophages were shown to up-regulate CDA level to induce gemcitabine resistance in PC cells (42). Functional impact of the gene expression changes was confirmed by demonstration of reduced intracellular accumulation of gemcitabine triphosphate in co-cultured PC cells, which was reversed by the inhibition of CXCR4 and/or hedgehog pathways. In contrast, we observed enhanced gemcitabine accrual in co-cultured PC cells, which significantly reduced upon CXCR4 and/or hedgehog inhibition. These findings establish a novel aspect of cooperative function of CXCR4 and hedgehog pathways in PC chemoresistance.

Our study also demonstrated that co-culture with PSCs led to reduced intracellular ROS levels in PC cells, which were restored upon targeted inhibition of CXCR4 and hedgehog pathways. Increased accumulation of ROS following drug treatment is an important mechanism of drug toxicity (43). Cancer cells, in general, have heightened levels of ROS because of increased metabolic demand of proliferating cells for quick energy and cellular building blocks (44). Increased ROS likely contributes to cancer pathogenesis via promotion of genetic instability and it also remodels ECM components by activating proteolytic enzymes in cancer cells, which help in tumor cell migration and dissemination (45, 46). However, to check the ROS levels beyond a threshold, tumor cells overexpress enzymes of the anti-oxidant system (46). Our findings provide evidence that tumor-stromal crosstalk mediated through CXCR4 and hedgehog pathways controls the expression of antioxidant genes (*NRF-2* and *GPX-1*). Earlier data suggest that

NRF-2 is highly expressed in pancreatic tumors and patients with low levels of NRF-2 are more sensitive to chemotherapy (47, 48). Furthermore, down-regulation of NRF-2 increases gemcitabine sensitivity of PC cells (47). GPX1, which counteracts oxidative stress, has oncogenic role in several malignancies. However, low GPX-1 expression has been correlated with poor survival rate of PC patients treated with gemcitabine (49). Recent finding suggested GPX-1 as an important regulator of glucose metabolism in PC cells (50). This clearly suggests complex and context dependent role of GPX-1 in cancer which needs to be addressed in great detail.

Cancer stemness is another important characteristic associated with the poor response of chemotherapy (51). Stemness potential of the cancer cells is controlled by certain transcription factors that regulate expression of genes associated with tumor maintenance, aggressiveness, and chemoresistance (52, 53). We observed increased expression of two important stem cell–associated transcription factors, SOX2 and OCT4, in PC cells co-cultured with PSCs, and targeting of CXCR4 and/or hedgehog pathways led to their reduced expression. SOX2 expression is shown to increase levels of pancreatic CSC markers and increase cell proliferation and stemness (54). Similarly, up-regulation of OCT4 maintains undifferentiated state of induced pluripotent stem cell state, whereas the loss of OCT4 induces differentiation of stem cells (55). Study suggested that inhibition of OCT4 and Nanog abolished stemness of pancreatic cancer cells (56). In some reports, a role of canonical hedgehog signaling in pancreatic CSCs and gemcitabine resistance has also been demonstrated (57, 58). In agreement, we also observed an up-regulation of SOX2 in PC cells treated with SHH, although treatment with CXCL12 imparted a greater effect.

In summary, our findings provide a novel mechanistic basis for PC chemoresistance where tumor-stromal crosstalk mediated through CXCR4 and hedgehog pathways plays an important role and co-targeting of these signaling nodes in a combination therapy will lead to superior synergistic clinical outcome in PC patients.

## Experimental procedures

### Cell lines and culture conditions

Pancreatic cancer cell lines MiaPaCa and Colo357 and PSCs were procured and maintained in culture as described previously (59, 60). Human pancreatic stellate cells were purchased from ScienCell Research Laboratories (Carlsbad, CA) and cultured according to their instructions. All the cells were routinely tested for mycoplasma contamination and authenticated intermittently using established markers either in house and/or by using a commercial service provider (Genetica DNA Laboratories, Burlington, NC and short-tandem repeats genotyping).

### Reagents and antibodies

The following reagents were used in this study: Dulbecco's Modified Eagle Medium (DMEM); Roswell Park Memorial Institute medium (RPMI 1640); fetal bovine serum (FBS) (Atlanta Biologicals, Lawrenceville, GA); penicillin and streptomycin (Invitrogen); High-Capacity RNA-to-cDNA™ Kit and SYBR Green Master Mix (Applied Biosystems, Carlsbad, CA); Western blotting SuperSignal West Femto Maximum sensitivity substrate kit (Thermo Scientific); EZ-Dewax (BioGenex, Fremont, CA); background sniper, polymer, and probe (Biocare Medical, Concord, CA); Plerixafor (AMD3100) and gemcitabine (Selleck Chemicals, Houston, TX); Vismodegib (GDC-0449) (LC Laboratories, Woburn, MA); LIVE/DEAD™ Viability/Cytotoxicity Kit (Thermo Fisher Scientific). The following antibodies were used: $\alpha$-cleaved PARP (rabbit polyclonal, Abcam, Cambridge, MA) and rabbit polyclonal cleaved caspas-3 (Cell Signaling Technology, Denver, MA), mouse monoclonal Ki67 (BD Biosciences), mouse monoclonal biotinylated anti–$\beta$-actin (Sigma-Aldrich), rabbit polyclonal $\alpha$-SMA (Epitomics, Burlingame, CA), rabbit polyclonal CXCR4 (Novus Biologicals, Centennial, CO), mouse monoclonal SMO (Millipore Sigma), and horseradish peroxidase (HRP)–labeled secondary antibodies (Santa Cruz Biotechnology).

### Cell co-culturing, treatments, and transfections

PCCs ($1.0 \times 10^5$cells/well) were seeded in the 6-well plates, whereas PSCs ($1.0 \times 10^5$cells/well) were seeded in 1-$\mu$m pore size insert chambers that were placed over PCCs. For monoculture controls, we seeded PCCs ($1.0 \times 10^5$ cells) in the insert chamber as well. Cells were kept in incubator for 48 h at 37 °C to establish co-culture, and thereafter, media were replaced and cells allowed to grow for additional 24 h and treated with AMD3100 (5 $\mu$g/ml) and GD-049 (5 $\mu$M) alone or together in presence and absence of gemcitabine (5 $\mu$M) for 24 to 96 h. For studies intended to estimate gemcitabine metabolites, gemcitabine treatment was given 4 h prior to cell harvesting. For knockdown of CXCR4 and SMO in pancreatic cancer and stellate cells, cells were cultured in 6-well plates and transfected with 100 nmol/liter of nontarget or ON-TARGETplus SMARTpool CXCR4 and SMO targeting siRNAs (Dharmacon, Lafayette, CO) using DharmaFECT (Dharmacon, Lafayette, CO) according to the manufacturer's instruction.

### Cell viability and sphere-formation assay

Pancreatic tumor cell growth was monitored by counting of number of viable cells on hemocytometer following staining with trypan blue. For sphere-formation assay, treated or untreated tumor cells were harvested, counted, and plated (1000 cells/well) in wells having ultra-low attachment surface. Culture inserts containing PCCs or PSCs were placed over plated cells. Spheres were visualized under microscope after 7 days and photographed.

### Measurement of reactive oxygen species

Intracellular reactive oxygen species (ROS) levels were determined as described earlier (11, 43). Briefly, cells from monoculture or co-culture were incubated with DCFDA dye in regular growth medium for 30 min at 37 °C and subsequently washed with PBS and resuspended in 400 $\mu$l PBS. Fluorescence intensity in cells was examined as a measure of ROS by flow cytometry on a FACSCanto IIi (BD Biosciences).

### RNA isolation and quantitative real time-PCR (qRT-PCR)

Total RNA was isolated by using TRIzol reagent, and 2 $\mu$g of RNA was taken for cDNA synthesis using the high-capacity

complementary DNA Reverse Transcription Kit following manufacturer's instructions. Subsequently, q-PCR was performed in 96-well plates using SYBR Green Master Mix, cDNA as a template, and specific primer pair sets (Table S3) on an iCycler system (Bio-Rad). The thermal conditions for real-time PCR assays were as follows: cycle 1: 95 °C for 10 min, cycle 2 (× 40): 95 °C for 10 s and 58–60 °C for 45 s.

### *Preparation of cell lysates and immunoblotting*

Total protein was isolated, estimated and processed for immunoblotting as described earlier (10, 61). Briefly, cell lysates were prepared in Nonidet P-40 lysis buffer and protein estimated using DC protein assay kit. Subsequently, 30 $\mu$g of protein was resolved on 10–12% polyacrylamide gels and transferred onto PVDF membranes. Blots were washed, blocked in 5% milk, and probed with primary antibody (1:1000) followed by incubation with secondary HRP antibody (1:2000). $\beta$-actin (1:20,000) was used as an internal control. The signal was detected by using Super Signal West Femto maximum sensitivity substrate kit on the ChemiDoc Imaging System (Bio-Rad).

### *Oil Red O staining*

Pancreatic stellate cells were stained with Oil Red O to determine their activation by visualizing lipid droplets using Lipid (Oil Red O) Staining Kit (BioVision, Milpitas, CA). The assay was performed according to the manufacturer's instruction, and images were taken under light microscope.

### *Immunohistochemical and histological analyses*

5-$\mu$m sections were cut from orthotopic tumor xenograft tissues and processed for H&E staining and immunohistochemistry as described previously (60). All the antibodies were used at 1:100 dilutions. Tumor tissue sections were visualized under microscope and photographed.

### *Measurement of gemcitabine metabolites*

Treated cells in monoculture or co-culture were homogenized 1:10 using a pellet pestle with buffer containing 50:50 acetonitrile: 10 mM PO4 buffer, pH 9.5, containing 25 $\mu$g/ml THU and 2 mg/ml EDTA. Samples were spiked with internal standard (10 $\mu$l of a spiking solution containing 50 $\mu$g/ml 5-CL-deoxyuridne and 5 $\mu$g/ml cytidine N15 triphosphate in DI water) and mixed well. After centrifugation for 5 min at 21,000 × *g*, the supernatant was transferred to autosampler vials and analyzed by LC-tandem MS (LC-MS/MS).

### *Orthotopic xenograft study in mice*

All animal experiments were performed under a protocol approved by the University of South Alabama Institutional Animal Care and Use Committee (IACUC). Immunocompromised nude mice (4–6 weeks old; Harlan Laboratories, Prattville, AL) were anesthetized with intraperitoneal (i.p.) injection of ketamine (100 mg/kg) and xylazine (15 mg/kg). A mixture (1:5) of luciferase-tagged pancreatic cancer cells ($1 \times 10^6$) and PSCs, human PSCs ($5 \times 10^6$) suspended in 100 $\mu$l normal saline was injected into the tail region of the pancreas as described previously (62). Once tumor became palpable (7th day post injection), mice were randomly divided into eight treatment groups (6 mice/group) and treatment initiated as listed (Table S4). Tumor growth was monitored biweekly by bioluminescence imaging using Xenogen-IVIS-cooled CCD optical system (IVIS Spectrum) following i.p. injection of D-Luciferin (150 mg/kg). At the end point, final imaging was performed, and animals sacrificed. Thereafter, tumors were resected and weighed, and their volumes measured using by the following formula: $(A \times B2)/2$, where $A$ is the larger and $B$ is the smaller of the two dimensions.

### *Statistical analysis*

All the experiments were performed at least three times in biological replicates and data expressed as mean ± S.D. Wherever appropriate, the data were also subjected to unpaired two-tailed Student's $t$ test and two-way ANOVA. *, $p < 0.05$ was considered as significant.

## Data availability

The data presented in this manuscript are stored with us and are available from Ajay Pratap Singh, asingh@health.southalabama.edu, for sharing upon a reasonable request.

*Acknowledgments*—We thank Dr. Joel Andrews, Manager, Bioimaging Core Facility at USAMCI, for assistance in microscopy analysis.

*Author contributions*—M. A. K., S. K. S., S. A., and G. S. G. data curation; M. A. K., S. K. S., J. E. C., G. S. G., and A. P. S. formal analysis; M. A. K. visualization; M. A. K., S. K. S., H. Z., and G. K. P. methodology; M. A. K., H. Z., and G. K. P. writing-original draft; M. A. K., S. K. S., H. Z., M. K., G. S. G., S. S., and A. P. S. writing-review and editing; S. A. investigation; S. S. and A. P. S. conceptualization; A. P. S. resources; A. P. S. supervision; A. P. S. funding acquisition; A. P. S. project administration.

*Funding and additional information*—This work was supported by NCI, National Institutes of Health Grants R01CA175772 and R01CA224306 (to A. P. S.). The content is solely the responsibility of the authors and does not necessarily represent the official views of the National Institutes of Health.

*Conflict of interest*—The authors declare that they have no conflicts of interest with the contents of this article.

*Abbreviations*—The abbreviations used are: PC, pancreatic cancer; Hh, hedgehog; PCC, pancreatic cancer cells; PSC, pancreatic stellate cell; ROS, reactive oxygen species; SHH, sonic hedgehog; PARP, poly (ADP-ribose) polymerase.

## References

1. Siegel, R. L., Miller, K. D., and Jemal, A. (2020) Cancer statistics, 2020. *CA Cancer J. Clin.* **70,** 7–30 CrossRef Medline
2. Aier, I., Semwal, R., Sharma, A., and Varadwaj, P. K. (2019) A systematic assessment of statistics, risk factors, and underlying features involved in pancreatic cancer. *Cancer Epidemiol.* **58,** 104–110 CrossRef Medline
3. Maitra, A., and Hruban, R. H. (2008) Pancreatic cancer. *Annu. Rev. Pathol.* **3,** 157–188 CrossRef Medline
4. Conroy, T., Desseigne, F., Ychou, M., Bouché, O., Guimbaud, R., Bécouarn, Y., Adenis, A., Raoul, J. L., Gourgou-Bourgade, S., de la Fouchardière, C., Bennouna, J., Bachet, J. B., Khemissa-Akouz, F., Péré-Vergé, D., Delbaldo, C., *et al.* (2011) FOLFIRINOX versus gemcitabine for metastatic pancreatic cancer. *N. Engl. J. Med.* **364,** 1817–1825 CrossRef Medline

5. Von Hoff, D. D., Ervin, T., Arena, F. P., Chiorean, E. G., Infante, J., Moore, M., Seay, T., Tjulandin, S. A., Ma, W. W., Saleh, M. N., Harris, M., Reni, M., Dowden, S., Laheru, D., Bahary, N., *et al.* (2013) Increased survival in pancreatic cancer with nab-paclitaxel plus gemcitabine. *N. Engl. J. Med.* **369,** 1691–1703 CrossRef Medline
6. Wang-Gillam, A., Li, C. P., Bodoky, G., Dean, A., Shan, Y. S., Jameson, G., Macarulla, T., Lee, K. H., Cunningham, D., Blanc, J. F., Hubner, R. A., Chiu, C. F., Schwartsmann, G., Siveke, J. T., Braiteh, F., *et al.* (2016) Nanoliposomal irinotecan with fluorouracil and folinic acid in metastatic pancreatic cancer after previous gemcitabine-based therapy (NAPOLI-1): A global, randomised, open-label, phase 3 trial. *Lancet* **387,** 545–557 CrossRef Medline
7. Fiorini, C., Cordani, M., Gotte, G., Picone, D., and Donadelli, M. (2015) Onconase induces autophagy sensitizing pancreatic cancer cells to gemcitabine and activates Akt/mTOR pathway in a ROS-dependent manner. *Biochim. Biophys. Acta* **1853,** 549–560 CrossRef Medline
8. Fiorini, C., Cordani, M., Padroni, C., Blandino, G., Di Agostino, S., and Donadelli, M. (2015) Mutant p53 stimulates chemoresistance of pancreatic adenocarcinoma cells to gemcitabine. *Biochim. Biophys. Acta* **1853,** 89–100 CrossRef Medline
9. Costantino, C. L., Witkiewicz, A. K., Kuwano, Y., Cozzitorto, J. A., Kennedy, E. P., Dasgupta, A., Keen, J. C., Yeo, C. J., Gorospe, M., and Brody, J. R. (2009) The role of HuR in gemcitabine efficacy in pancreatic cancer: HuR Up-regulates the expression of the gemcitabine metabolizing enzyme deoxycytidine kinase. *Cancer Res.* **69,** 4567–4572 CrossRef Medline
10. Arora, S., Bhardwaj, A., Singh, S., Srivastava, S. K., McClellan, S., Nirodi, C. S., Piazza, G. A., Grizzle, W. E., Owen, L. B., and Singh, A. P. (2013) An undesired effect of chemotherapy: gemcitabine promotes pancreatic cancer cell invasiveness through reactive oxygen species-dependent, nuclear factor κB- and hypoxia-inducible factor 1α-mediated up-regulation of CXCR4. *J. Biol. Chem.* **288,** 21197–21207 CrossRef Medline
11. Patel, G. K., Khan, M. A., Bhardwaj, A., Srivastava, S. K., Zubair, H., Patton, M. C., Singh, S., Khushman, M., and Singh, A. P. (2017) Exosomes confer chemoresistance to pancreatic cancer cells by promoting ROS detoxification and miR-155-mediated suppression of key gemcitabine-metabolising enzyme, DCK. *Br. J. Cancer* **116,** 609–619 CrossRef Medline
12. Ju, H. Q., Gocho, T., Aguilar, M., Wu, M., Zhuang, Z. N., Fu, J., Yanaga, K., Huang, P., and Chiao, P. J. (2015) Mechanisms of overcoming intrinsic resistance to gemcitabine in pancreatic ductal adenocarcinoma through the redox modulation. *Mol. Cancer Ther.* **14,** 788–798 CrossRef Medline
13. Ansari, D., Ohlsson, H., Althini, C., Bauden, M., Zhou, Q., Hu, D., and Andersson, R. (2019) The Hippo signaling pathway in pancreatic cancer. *Anticancer Res.* **39,** 3317–3321 CrossRef Medline
14. Chen, F., Long, Q., Fu, D., Zhu, D., Ji, Y., Han, L., Zhang, B., Xu, Q., Liu, B., Li, Y., Wu, S., Yang, C., Qian, M., Xu, J., Liu, S., *et al.* (2018) Targeting SPINK1 in the damaged tumour microenvironment alleviates therapeutic resistance. *Nat. Commun.* **9,** 4315 CrossRef Medline
15. Miyamoto, H., Murakami, T., Tsuchida, K., Sugino, H., Miyake, H., and Tashiro, S. (2004) Tumor-stroma interaction of human pancreatic cancer: Acquired resistance to anticancer drugs and proliferation regulation is dependent on extracellular matrix proteins. *Pancreas* **28,** 38–44 CrossRef Medline
16. von Ahrens, D., Bhagat, T. D., Nagrath, D., Maitra, A., and Verma, A. (2017) The role of stromal cancer-associated fibroblasts in pancreatic cancer. *J. Hematol. Oncol* **10,** 76 CrossRef Medline
17. Thomas, D., and Radhakrishnan, P. (2019) Tumor-stromal crosstalk in pancreatic cancer and tissue fibrosis. *Mol. Cancer* **18,** 14 CrossRef Medline
18. Bailey, J. M., Swanson, B. J., Hamada, T., Eggers, J. P., Singh, P. K., Caffery, T., Ouellette, M. M., and Hollingsworth, M. A. (2008) Sonic hedgehog promotes desmoplasia in pancreatic cancer. *Clin. Cancer Res.* **14,** 5995–6004 CrossRef Medline
19. Ene-Obong, A., Clear, A. J., Watt, J., Wang, J., Fatah, R., Riches, J. C., Marshall, J. F., Chin-Aleong, J., Chelala, C., Gribben, J. G., Ramsay, A. G., and Kocher, H. M. (2013) Activated pancreatic stellate cells sequester $CD8^+$ T cells to reduce their infiltration of the juxtatumoral compartment of pancreatic ductal adenocarcinoma. *Gastroenterology* **145,** 1121–1132 CrossRef Medline
20. Singh, S., Srivastava, S. K., Bhardwaj, A., Owen, L. B., and Singh, A. P. (2010) CXCL12-CXCR4 signalling axis confers gemcitabine resistance to pancreatic cancer cells: A novel target for therapy. *Br. J. Cancer* **103,** 1671–1679 CrossRef Medline
21. Singh, A. P., Arora, S., Bhardwaj, A., Srivastava, S. K., Kadakia, M. P., Wang, B., Grizzle, W. E., Owen, L. B., and Singh, S. (2012) CXCL12/CXCR4 protein signaling axis induces sonic hedgehog expression in pancreatic cancer cells via extracellular regulated kinase- and Akt kinase-mediated activation of nuclear factor κB: Implications for bidirectional tumor-stromal interactions. *J. Biol. Chem.* **287,** 39115–39124 CrossRef Medline
22. Neesse, A., Bauer, C. A., Öhlund, D., Lauth, M., Buchholz, M., Michl, P., Tuveson, D. A., and Gress, T. M. (2019) Stromal biology and therapy in pancreatic cancer: Ready for clinical translation? *Gut* **68,** 159–171 CrossRef Medline
23. Olive, K. P., Jacobetz, M. A., Davidson, C. J., Gopinathan, A., McIntyre, D., Honess, D., Madhu, B., Goldgraben, M. A., Caldwell, M. E., Allard, D., Frese, K. K., Denicola, G., Feig, C., Combs, C., Winter, S. P., *et al.* (2009) Inhibition of hedgehog signaling enhances delivery of chemotherapy in a mouse model of pancreatic cancer. *Science* **324,** 1457–1461 CrossRef Medline
24. Allison, M. (2012) Hedgehog hopes lifted by approval . . . and stung by failure. *Nat. Biotechnol.* **30,** 203 CrossRef Medline
25. Rhim, A. D., Oberstein, P. E., Thomas, D. H., Mirek, E. T., Palermo, C. F., Sastra, S. A., Dekleva, E. N., Saunders, T., Becerra, C. P., Tattersall, I. W., Westphalen, C. B., Kitajewski, J., Fernandez-Barrena, M. G., Fernandez-Zapico, M. E., Iacobuzio-Donahue, C., Olive, K. P., and Stanger, B. Z. (2014) Stromal elements act to restrain, rather than support, pancreatic ductal adenocarcinoma. *Cancer Cell* **25,** 735–747 CrossRef Medline
26. Özdemir, B. C., Pentcheva-Hoang, T., Carstens, J. L., Zheng, X., Wu, C. C., Simpson, T. R., Laklai, H., Sugimoto, H., Kahlert, C., Novitskiy, S. V., De Jesus-Acosta, A., Sharma, P., Heidari, P., Mahmood, U., Chin, L., *et al.* (2014) Depletion of carcinoma-associated fibroblasts and fibrosis induces immunosuppression and accelerates pancreas cancer with reduced survival. *Cancer Cell* **25,** 719–734 CrossRef Medline
27. Saur, D., Seidler, B., Schneider, G., Algül, H., Beck, R., Senekowitsch-Schmidtke, R., Schwaiger, M., and Schmid, R. M. (2005) CXCR4 expression increases liver and lung metastasis in a mouse model of pancreatic cancer. *Gastroenterology* **129,** 1237–1250 CrossRef Medline
28. Wang, Z., Ma, Q., Li, P., Sha, H., Li, X., and Xu, J. (2013) Aberrant expression of CXCR4 and β-catenin in pancreatic cancer. *Anticancer Res.* **33,** 4103–4110 Medline
29. Zhang, J., Liu, C., Mo, X., Shi, H., and Li, S. (2018) Mechanisms by which CXCR4/CXCL12 cause metastatic behavior in pancreatic cancer. *Oncol. Lett.* **15,** 1771–1776 CrossRef Medline
30. Li, X., Wang, Z., Ma, Q., Xu, Q., Liu, H., Duan, W., Lei, J., Ma, J., Wang, X., Lv, S., Han, L., Li, W., Guo, J., Guo, K., Zhang, D., Wu, E., and Xie, K. (2014) Sonic hedgehog paracrine signaling activates stromal cells to promote perineural invasion in pancreatic cancer. *Clin. Cancer Res.* **20,** 4326–4338 CrossRef Medline
31. Xiao, G., Wang, X., and Yu, Y. (2017) CXCR4/Let-7a axis regulates metastasis and chemoresistance of pancreatic cancer cells through targeting hmga2. *Cell Physiol. Biochem.* **43,** 840–851 CrossRef Medline
32. Khan, M. A., Azim, S., Zubair, H., Bhardwaj, A., Patel, G. K., Khushman, M., Singh, S., and Singh, A. P. (2017) Molecular drivers of pancreatic cancer pathogenesis: Looking inward to move forward. *Int. J. Mol. Sci.* **18,** E779 CrossRef Medline
33. Tu, Y., Niu, M., Xie, P., Yue, C., Liu, N., Qi, Z., Gao, S., Liu, H., Shi, Q., Yu, R., and Liu, X. (2017) Smoothened is a poor prognosis factor and a potential therapeutic target in glioma. *Sci. Rep.* **7,** 42630 CrossRef Medline
34. Righi, E., Kashiwagi, S., Yuan, J., Santosuosso, M., Leblanc, P., Ingraham, R., Forbes, B., Edelblute, B., Collette, B., Xing, D., Kowalski, M., Mingari, M. C., Vianello, F., Birrer, M., Orsulic, S., Dranoff, G., and Poznansky, M. C. (2011) CXCL12/CXCR4 blockade induces multimodal antitumor effects that prolong survival in an immunocompetent mouse model of ovarian cancer. *Cancer Res.* **71,** 5522–5534 CrossRef Medline
35. Saiki, Y., Yoshino, Y., Fujimura, H., Manabe, T., Kudo, Y., Shimada, M., Mano, N., Nakano, T., Lee, Y., Shimizu, S., Oba, S., Fujiwara, S., Shimizu,

H., Chen, N., Nezhad, Z. K., *et al.* (2012) DCK is frequently inactivated in acquired gemcitabine-resistant human cancer cells. *Biochem. Biophys. Res. Commun.* **421,** 98–104 CrossRef Medline
36. Xiong, J., Altaf, K., Ke, N., Wang, Y., Tang, J., Tan, C., Li, A., Zhang, H., He, D., and Liu, X. (2016) dCK expression and gene polymorphism with gemcitabine chemosensitivity in patients with pancreatic ductal adenocarcinoma: A strobe-compliant observational study. *Medicine* (*Baltimore*) **95,** e2936 CrossRef Medline
37. Hu, Q., Qin, Y., Xiang, J., Liu, W., Xu, W., Sun, Q., Ji, S., Liu, J., Zhang, Z., Ni, Q., Xu, J., Yu, X., and Zhang, B. (2018) dCK negatively regulates the NRF2/ARE axis and ROS production in pancreatic cancer. *Cell Prolif.* **51,** e12456 CrossRef Medline
38. Hunsucker, S. A., Spychala, J., and Mitchell, B. S. (2001) Human cytosolic 5′-nucleotidase I: Characterization and role in nucleoside analog resistance. *J. Biol. Chem.* **276,** 10498–10504 CrossRef Medline
39. Patzak, M. S., Kari, V., Patil, S., Hamdan, F. H., Goetze, R. G., Brunner, M., Gaedcke, J., Kitz, J., Jodrell, D. I., Richards, F. M., Pilarsky, C., Gruetzmann, R., Rümmele, P., Knösel, T., Hessmann, E., Ellenrieder, V., Johnsen, S. A., and Neesse, A. (2019) Cytosolic 5′-nucleotidase 1A is overexpressed in pancreatic cancer and mediates gemcitabine resistance by reducing intracellular gemcitabine metabolites. *EBioMedicine* **40,** 394–405 CrossRef Medline
40. Amrutkar, M., and Gladhaug, I. P. (2017) Pancreatic cancer chemoresistance to gemcitabine. *Cancers* (*Basel*) **9,** E157 CrossRef Medline
41. Frese, K. K., Neesse, A., Cook, N., Bapiro, T. E., Lolkema, M. P., Jodrell, D. I., and Tuveson, D. A. (2012) nab-Paclitaxel potentiates gemcitabine activity by reducing cytidine deaminase levels in a mouse model of pancreatic cancer. *Cancer Discov.* **2,** 260–269 CrossRef Medline
42. Weizman, N., Krelin, Y., Shabtay-Orbach, A., Amit, M., Binenbaum, Y., Wong, R. J., and Gil, Z. (2014) Macrophages mediate gemcitabine resistance of pancreatic adenocarcinoma by upregulating cytidine deaminase. *Oncogene* **33,** 3812–3819 CrossRef Medline
43. Khan, M. A., Gahlot, S., and Majumdar, S. (2012) Oxidative stress induced by curcumin promotes the death of cutaneous T-cell lymphoma (HuT-78) by disrupting the function of several molecular targets. *Mol. Cancer Ther.* **11,** 1873–1883 CrossRef Medline
44. Kumari, S., Badana, A. K., G, M. M., G, S., Malla, R. (2018) Reactive oxygen species: A key constituent in cancer survival. *Biomark Insights* **13,** 1177271918755391 CrossRef Medline
45. Nikitovic, D., Corsini, E., Kouretas, D., Tsatsakis, A., and Tzanakakis, G. (2013) ROS-major mediators of extracellular matrix remodeling during tumor progression. *Food Chem. Toxicol.* **61,** 178–186 CrossRef Medline
46. Schumacker, P. T. (2006) Reactive oxygen species in cancer cells: Live by the sword, die by the sword. *Cancer Cell* **10,** 175–176 CrossRef Medline
47. Lister, A., Nedjadi, T., Kitteringham, N. R., Campbell, F., Costello, E., Lloyd, B., Copple, I. M., Williams, S., Owen, A., Neoptolemos, J. P., Goldring, C. E., and Park, B. K. (2011) Nrf2 is overexpressed in pancreatic cancer: Implications for cell proliferation and therapy. *Mol. Cancer* **10,** 37 CrossRef Medline
48. Soini, Y., Eskelinen, M., Juvonen, P., Kärjä, V., Haapasaari, K. M., Saarela, A., and Karihtala, P. (2014) Nuclear Nrf2 expression is related to a poor survival in pancreatic adenocarcinoma. *Pathol. Res. Pract.* **210,** 35–39 CrossRef Medline
49. Meng, Q., Shi, S., Liang, C., Liang, D., Hua, J., Zhang, B., Xu, J., and Yu, X. (2018) Abrogation of glutathione peroxidase-1 drives EMT and chemoresistance in pancreatic cancer by activating ROS-mediated Akt/GSK3β/Snail signaling. *Oncogene* **37,** 5843–5857 CrossRef Medline
50. Meng, Q., Xu, J., Liang, C., Liu, J., Hua, J., Zhang, Y., Ni, Q., Shi, S., and Yu, X. (2018) GPx1 is involved in the induction of protective autophagy in pancreatic cancer cells in response to glucose deprivation. *Cell Death Dis.* **9,** 1187 CrossRef Medline
51. Nunes, T., Hamdan, D., Leboeuf, C., El Bouchtaoui, M., Gapihan, G., Nguyen, T. T., Meles, S., Angeli, E., Ratajczak, P., Lu, H., Di Benedetto, M., Bousquet, G., and Janin, A. (2018) Targeting cancer stem cells to overcome chemoresistance. *Int. J. Mol. Sci.* **19,** E4036 CrossRef Medline
52. Deshmukh, S. K., Srivastava, S. K., Zubair, H., Bhardwaj, A., Tyagi, N., Al-Ghadhban, A., Singh, A. P., Dyess, D. L., Carter, J. E., and Singh, S. (2017) Resistin potentiates chemoresistance and stemness of breast cancer cells: Implications for racially disparate therapeutic outcomes. *Cancer Lett.* **396,** 21–29 CrossRef Medline
53. Zubair, H., Azim, S., Srivastava, S. K., Bhardwaj, A., Marimuthu, S., Patton, M. C., Singh, S., and Singh, A. P. (2016) Cancer stem cells: Concept, significance, and management. in *Stem Cells in Toxicology and Medicine* (Sahu, S. C., ed) pp. 375–413, John Wiley & Sons, Ltd, Chichester, UK
54. Herreros-Villanueva, M., Zhang, J. S., Koenig, A., Abel, E. V., Smyrk, T. C., Bamlet, W. R., de Narvajas, A. A., Gomez, T. S., Simeone, D. M., Bujanda, L., and Billadeau, D. D. (2013) SOX2 promotes dedifferentiation and imparts stem cell-like features to pancreatic cancer cells. *Oncogenesis* **2,** e61 CrossRef Medline
55. Herreros-Villanueva, M., Bujanda, L., Billadeau, D. D., and Zhang, J. S. (2014) Embryonic stem cell factors and pancreatic cancer. *World J. Gastroenterol.* **20,** 2247–2254 CrossRef Medline
56. Lu, Y., Zhu, H., Shan, H., Lu, J., Chang, X., Li, X., Lu, J., Fan, X., Zhu, S., Wang, Y., Guo, Q., Wang, L., Huang, Y., Zhu, M., and Wang, Z. (2013) Knockdown of Oct4 and Nanog expression inhibits the stemness of pancreatic cancer cells. *Cancer Lett.* **340,** 113–123 CrossRef Medline
57. Fu, J., Rodova, M., Roy, S. K., Sharma, J., Singh, K. P., Srivastava, R. K., and Shankar, S. (2013) GANT-61 inhibits pancreatic cancer stem cell growth in vitro and in NOD/SCID/IL2R gamma null mice xenograft. *Cancer Lett.* **330,** 22–32 CrossRef Medline
58. Singh, B. N., Fu, J., Srivastava, R. K., and Shankar, S. (2011) Hedgehog signaling antagonist GDC-0449 (Vismodegib) inhibits pancreatic cancer stem cell characteristics: Molecular mechanisms. *PLoS One* **6,** e27306 CrossRef Medline
59. Zubair, H., Azim, S., Srivastava, S. K., Ahmad, A., Bhardwaj, A., Khan, M. A., Patel, G. K., Arora, S., Carter, J. E., Singh, S., and Singh, A. P. (2016) Glucose metabolism reprogrammed by overexpression of IKKε promotes pancreatic tumor growth. *Cancer Res.* **76,** 7254–7264 CrossRef Medline
60. Bhardwaj, A., Srivastava, S. K., Singh, S., Tyagi, N., Arora, S., Carter, J. E., Khushman, M., and Singh, A. P. (2016) MYB promotes desmoplasia in pancreatic cancer through direct transcriptional up-regulation and cooperative action of sonic hedgehog and adrenomedullin. *J. Biol. Chem.* **291,** 16263–16270 CrossRef Medline
61. Khan, M. A., Srivastava, S. K., Bhardwaj, A., Singh, S., Arora, S., Zubair, H., Carter, J. E., and Singh, A. P. (2015) Gemcitabine triggers angiogenesis-promoting molecular signals in pancreatic cancer cells: Therapeutic implications. *Oncotarget* **6,** 39140–39150 CrossRef Medline
62. Aiello, N. M., Rhim, A. D., and Stanger, B. Z. (2016) Orthotopic injection of pancreatic cancer cells. *Cold Spring Harb Protoc.* **2016,** pdb.prot078360 CrossRef Medline